

# Preparation and Characterization of Hydroxyapatite-Poly(Vinyl Alcohol) Composites Reinforced with Cellulose Nanocrystals

Wenbang Wei,<sup>a,b,c,d</sup> Wei Song,<sup>a,b,c</sup> and Shuangbao Zhang<sup>a,b,c,\*</sup>

Hydroxyapatite/poly(vinyl alcohol) (HAp/PVA) composites have been proposed as a promising biomaterial for use in articular cartilage repair. In this study, HAp/PVA composite gels reinforced with cellulose nanocrystals (CNC) were prepared using the freeze/thaw method. The influence of CNC as a reinforcement on the structure of composite gels was investigated *via* Fourier transform infrared spectroscopy (FT-IR), X-ray powder diffraction (XRD), and scanning electron microscopy (SEM). The mechanical properties and thermal stability of the composite gels were also studied. The FT-IR and XRD results indicated that the HAp/PVA/CNC composite gels were formed by hydrogen bonding. SEM morphology showed that the CNC served as an enhancement phase that interpenetrated the network of the HAp/PVA composite gels. The tensile strength and tensile modulus of the composites improved with increasing dosage of CNC. The thermal stability measurements indicated that the thermal stability of the HAp/PVA composites was slightly improved with the addition of the CNC.

*Keywords:* Preparation and characterization; HAp/PVA composite gels; Cellulose nanocrystals; Reinforcement; Articular cartilage repair

*Contact information:* a: MOE Key Laboratory of Wooden Material Science and Application, College of Materials Science and Technology, Beijing Forestry University, 100083, Beijing, China; b: Beijing Key Laboratory of Wood Science and Engineering, College of Materials Science and Technology, Beijing Forestry University, 100083, Beijing, China; c: MOE Engineering Research Center of Forestry Biomass Materials and Bioenergy, College of Materials Science and Technology, Beijing Forestry University, 100083, Beijing, China; d: Guangxi Eco-engineering Vocational and Technical College, 545004, Liuzhou, China; \*Corresponding author: shuangbaozhang@126.com

## INTRODUCTION

Poly(vinyl alcohol) (PVA) gel is widely used in the biomedical fields due to its excellent biocompatibility, having such applications as soft tissue replacement, drug delivery, and the construction of hemodialysis membranes (Hyon *et al.* 1989). PVA gel possesses excellent chemical resistance and has several advantages, including easy preparation, appropriate physical properties, good biocompatibility, and low price. Especially important, it has a high moisture content and shows good lubrication as well as bio-tribological properties. Accordingly, increasing attention has been paid to the preparation of environmentally compatible PVA-based materials for a wide range of applications (Chiellini *et al.* 2003). However, the major challenge of using PVA hydrogel in clinical applications is that of fixation within the natural tissue. Since PVA hydrogel itself does not adhere to tissue due to its nonbioactivity, the long-term fixation of PVA hydrogel implants by way of suture is difficult (Stammen *et al.* 2001).

Around 60% of bone is made up of nano-scale hydroxyapatite (HAp), which has been widely used as a major component of composite materials in medical applications such as bone tissue engineering due to its excellent bioactive and biocompatibility properties (Huang *et al.* 1997; Ahn *et al.* 2001). Recent research has suggested that synthetic HAp may even more closely resemble bone minerals in composition, size, and morphology, thus permitting better osteoconductivity to be achieved (Du *et al.* 1999). Furthermore, the use of the synthetic version as a substitute for articular cartilage is expected to improve the mechanical properties of the articular structure due to the high load bearing properties of the synthetic. Moreover, the synthetic material is able to bond with the natural bone tissue through an osteo-conduction mechanism (Arvind *et al.* 2007).

The biocompatibility and biodegradability of natural polymers are essential for tissue engineering; therefore, the HAp/PVA composite gels must be carefully prepared to cultivate their excellent bioactivities and incorporate the nanotopographic features that mimic the nanostructure of bone (Swetha *et al.* 2010). For example, as cells are naturally accustomed to interacting with nano-structured surface roughness in the body, polymers can be modified to duplicate such a roughness through the incorporation of nanophase materials (Balasundaram and Webster 2007). However, the mechanical and thermal properties of the HAp/PVA composite gels could be improved by incorporating the nanocomposites.

Cellulose nanocrystals (CNC) are a promising example of such materials and have been widely studied over the past two decades. A broad range of uses for CNC, such as in structural plastics, smart coatings, cosmetics, pharmaceuticals, and solar energy collection, has been speculated for use in industry (Habibi *et al.* 2010; Eichhorn 2011). These CNC particles are commonly prepared by way of strong acid hydrolysis (Azizi Samir *et al.* 2005).

At present, CNC-based composites with both natural and synthetic polymers are being used as matrices to improve the mechanical and thermal properties of the resulting nanocomposites (Azizi Samir *et al.* 2004; Siqueira *et al.* 2009). These improved properties of CNC nanocomposites are primarily due to the extensive hydrogen bonding or chemical interactions between the CNC and polymer matrices (Azizi Samir *et al.* 2004; Candanedo *et al.* 2005). To our best knowledge, the incorporation of CNC into the HAp/PVA composite gels has not been reported.

HAp/PVA composite gels have been studied extensively (Pan *et al.* 2007; Pan and Xiong 2010; Gonzalez and Alvarez 2014; Sun and Uyama 2014); however, the application of CNC as the fiber-reinforced phase in HAp/PVA composite gels has not been reported.

The major goal of the present study was to prepare a new biomaterial for use as an articular cartilage replacement and to develop biodegradable HAp/PVA/CNC composite gels by way of an inexpensive and facile method (the freeze-thaw crosslinking method) to mimic the topological structure of human bone tissue. The effects of CNC incorporation on the chemical and morphological properties of the HAp/PVA composites were fully investigated using Fourier transform infrared spectrometry (FT-IR), X-ray powder diffraction (XRD), and scanning electron microscopy (SEM), and their mechanical properties and thermal stability were also studied.

## EXPERIMENTAL

### Materials

#### *Raw materials*

The PVA, which was purchased from Shanghai Chemical Co., Ltd, was found to have a saponification degree of 99% and a number-average polymerization degree of  $1750 \pm 50$ . *Eucalyptus* pulp fibers were supplied by the LiuJiang Pulp Factory, China. Sulfuric acid (98 wt%) was obtained from Beijing Chemical Reagent Factory, China.  $\text{CaCl}_2$ ,  $\text{NH}_3 \cdot \text{H}_2\text{O}$ , and  $(\text{NH}_4)_2\text{HPO}_4$  were obtained from Sinopharm Chemical Reagent Co., Ltd. All chemicals were used without any further purification.

#### *CNC preparation*

The pulp fibers were treated with  $\text{NaClO}_2$  in an acidic solution (pH = 3.8 to 4.0, adjusted with acetic acid) at 70 °C for 2 h. Next, the purified pulp fibers were filtered and washed thoroughly with distilled water and then oven dried overnight. The fibers (5 g) were cut into small pieces and hydrolyzed with a 50 wt%  $\text{H}_2\text{SO}_4$  solution (200 mL) in a water bath at 50 °C for 2 h under constant stirring. After the hydrolysis, the dispersions were washed three times with deionized water via centrifugation. Then the sample was dialyzed against deionized water until the pH of the dispersion was 6. The CNC suspension was stored in a refrigerator at 5 °C prior to use. The final CNC yield was 56% (Yield=Dried CNC/Dried pulp fiber).

#### *HAp preparation*

The  $\text{CaCl}_2$  solution was added dropwise into the  $(\text{NH}_4)_2\text{H}(\text{PO}_4)_2$  solution, and the pH was controlled in the range of 9 and 10 using a 1.0 M  $\text{NH}_3 \cdot \text{H}_2\text{O}$  solution. After the  $\text{CaCl}_2$  solution had been completely added, the mixtures were stirred vigorously for 2.5 h. Following decantation, the precipitates were washed for three consecutive times with deionized water, and then the HAp precursor was aged at 75 °C for 12 h. The obtained dry particles were ground using a pestle before being subjected to calcination at 600 °C. The quantities of the reactants were selected so as to provide a Ca/P molar ratio of 1.67 (He *et al.* 2012).

#### *Preparation of nano-HAp/PVA/CNC composite gels*

In a typical run, an aqueous 10% PVA solution was prepared by dissolving PVA in deionized water and then heating it at 90 °C for 2 h. The desired amounts of HAp powder were dissolved into the ethanol solution via sonication. Next, the 2% HAp solution was mixed into the PVA solution, and then the solutions were stirred vigorously at 80 °C for 2 h until they had been homogeneously mixed. The suspension of CNC was prepared by means of approximately 5 min of sonication before the synthesis of composite gels was begun. The desired amounts of CNC were blended with the slurry under constant string. The same procedure was repeated for the CNC concentrations of 2.5, 3.75, 5.0, and 6.25 wt%, and the preparations obtained were noted as HAp/PVA/CNC-2.5, HAp/PVA/CNC-3.75, HAp/PVA/CNC-5.0, and HAp/PVA/CNC-6.25, respectively. The HAp/PVA/CNC-0 without CNC additives but prepared by the same procedure was used as a control sample. Finally, the solutions were poured into a stainless steel container and then subjected to three repeated freeze/thaw cycles. In each cycle, the sample was frozen at about -20 °C for 12 h and then thawed at room temperature for 6 h (Wu *et al.* 2008). After three freezing and thawing circles, the test

specimens were removed from the molded plates. They were then cleaned in an ultrasonic bath containing distilled water and dried in air at room temperature for 48 h. For mechanical measurements, the wet samples were dehydrated to constant weight at room temperature until their polymer/water weight ratio was equal to that of initial gel compositions. For the other measurements, the dried samples were prepared by drying the wet hydrogels under vacuum at 75 °C for 48 h.

## Analytical Methods

### *Atomic force microscopy (AFM) measurement*

The AFM measurement was conducted by depositing an aqueous dispersion of the CNC (0.1 mg/mL<sup>-1</sup>) on a freshly cleaved mica surface and dried at 60 °C under vacuum for 24 h. A JPK SPM Control Station III with a NanoWizard II stand-alone atomic force microscope (AFM) head was used to acquire images in tapping mode. All micrographs were presented in top-view with no filtering to ensure that all images were produced with the same quality.

### *Fourier transform infrared spectroscopy (FT-IR) measurement*

FT-IR spectra were obtained using a Perkin-Elmer System 1000 Fourier transform infrared spectrometer. Approximately 1 mg of the dried sample was mixed with 300 mg of dry KBr powder and then ground using an agate mortar and pestle. FT-IR spectra were collected over the range of 4000 to 700 cm<sup>-1</sup>.

### *Scanning electron microscopy (SEM) measurement*

The SEM examination was conducted using a scanning electron microscope (SEM, S2150, Hitachi, Japan) at an accelerating voltage of 10 kV. The surface of the dried sample was coated with a thin layer of platinum prior to examination.

### *X-ray diffraction (XRD) measurement*

The phase composition was examined *via* X-ray diffraction (XRD, DX-2500 diffractometer, China). Cu K $\alpha$  radiation, at a voltage of 40 kV and a current of 30 mA, was used for the diffraction. The powder of dried samples was aligned at 1° to the incident beam. A step size of 0.02° (2 $\theta$ ) and a scan speed of 3° min<sup>-1</sup> were used, and the diffraction data were collected from 5° to 45° (2 $\theta$ ).

### *Mechanical property measurement*

The mechanical properties of the rectangular wet specimens were evaluated using a universal mechanical tester (Instron-4465, Instron Corp., USA) at room temperature (25±1 °C). The gauge length were 20 mm, and specimen size=2×30×6 mm. The tests were conducted at a constant strain rate of 1 mm/min. The tensile strength and elongation at break were recorded, and the modulus was calculated from the increase in load detected from an elongation of 50 to 100%. Each wet sample was measured in triplicate to ensure the standard deviation ( $\leq 5\%$ ) in the stress-strain curves.

### *Thermal stability measurement*

The thermogravimetric studies were carried out on a simultaneous thermal analyzer (DTG-60, Shimadzu, Japan). All dried samples (45 °C, 24 h) were analyzed from room temperature to 600 °C at 20 °C/min in a nitrogen atmosphere and at a flow rate of 30 mL/min.

## RESULTS AND DISCUSSION

### Synthesis of HAp/PVA/CNC Composite Gels

The synthesis of the HAp/PVA/CNC composite gels consisted of the preparation of the HAp/PVA composites and then the manufacture of different samples by varying the concentration of CNC in the feed mixture of the composite between 2.5 and 6.25 wt%. A typical photo of a CNC-HAp/PVA composite gel is shown in Fig. 1. In order to avoid HAp particle agglomeration and enhance the performance of the HAp/PVA composites, the proportion of HAp used in the composite gels was controlled closely and considered a very critical parameter (Ma *et al.* 2010; Zhang *et al.* 2010). It has been demonstrated that excess HAp particles do not distribute well within the PVA polymer, readily weakening the interaction between HAp and PVA. Thus, the proportion of HAp particles added into the PVA solution for the synthesis of the HAp/PVA composite gels was only 2%. The AFM image of the acid-hydrolyzed CNC is shown in Fig. 2. The CNC had an average length of 178 nm, a diameter of 37 nm, and therefore an aspect ratio (the ratio of length to diameter) of ~5.



**Fig. 1.** The optical image of 2.5% CNC-HAp/PVA composite gels

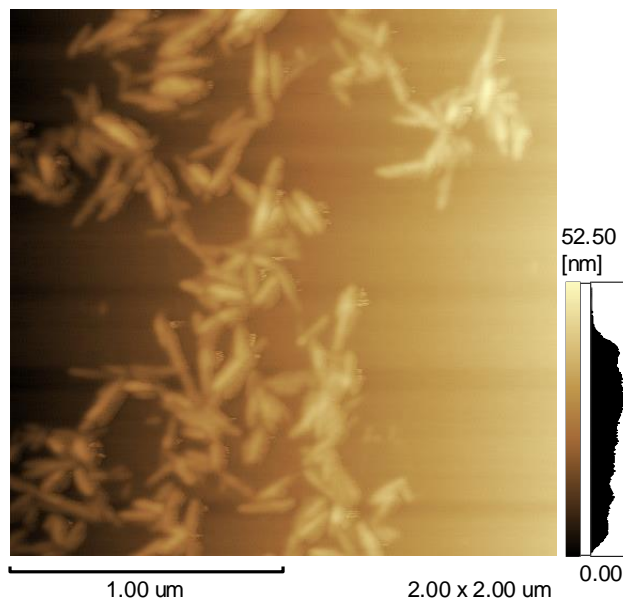


**Fig. 2.** Atomic force microscopy of the hydrolyzed CNC

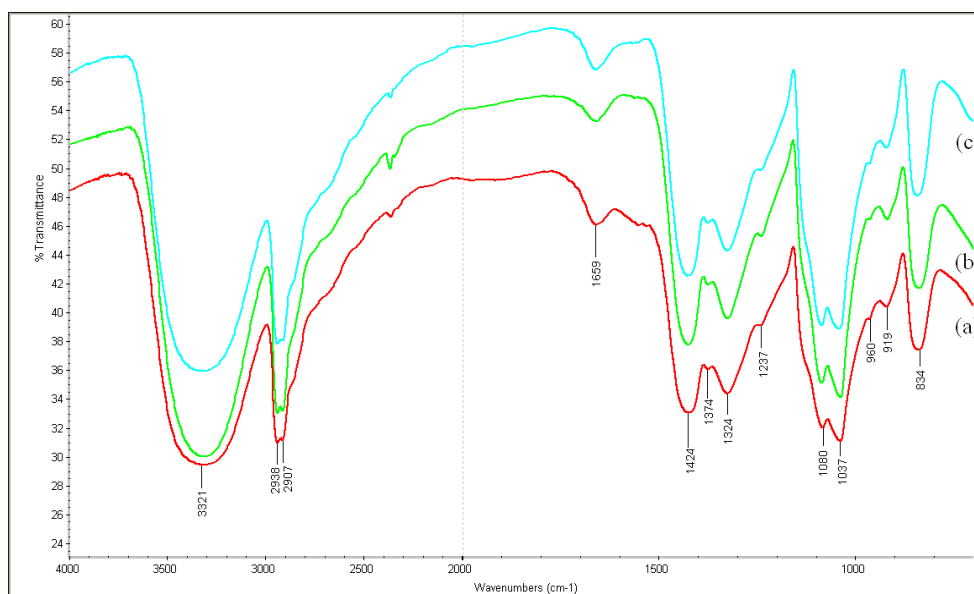


**Fig. 3.** FT-IR spectra of different composite gels as a function of CNC concentration. (a) represents the 0% CNC-HAp/PVA composite gels; (b) represents the 3.75% CNC-HAp/PVA composite gels; and (c) represents the 6.25% CNC-HAp/PVA composite gels.

### FT-IR Spectra Measurement

The interaction between inorganic and organic substances in the composite gels was studied using FT-IR spectra (Fig. 3). The large bands at 3300 to 3500  $\text{cm}^{-1}$  (assigned to O-H stretching vibrations) and near 2900  $\text{cm}^{-1}$  (assigned to C-H stretching vibrations) were observed for all the composite gels. The intensity of all these peaks changed slightly with the increase of the amount of CNC, indicating that the presence of CNC in the composites did not lead to chemical covalent bonding between the constituent phases, but rather probably shaped the physical hydrogen bonding that occurred in the composites, or, serving as an enhancement phase, physically interlocked the constituent phases, forming a three-dimensional structure that was formulated in an effort to improve material properties (Bhattacharya and Misra 2004). Furthermore, in the fingerprint region of 800 to 1500  $\text{cm}^{-1}$ , the majority of the peaks for the CNC were observed for all the samples. These results suggested that the presence of CNC in the composite gels did not influence their chemical structure (He *et al.* 2012). The broad bands at 1659  $\text{cm}^{-1}$  were due to the absorbed water on the surface of the hydrogels. The absorption at around 1430 to 1200  $\text{cm}^{-1}$  might have originated from C-H bend and C-C stretching. In addition, the bands at 1080, 1037, and 960  $\text{cm}^{-1}$  were probably due to the  $\text{PO}_4^{3-}$  stretching modes from the HAp crystalline structure (Pushpakanth *et al.* 2008). No significant peak change as a result of the composite gels was observed in the spectra for any group, which confirmed that the HAp/PVA/CNC composite gels were only mixtures and that no chemical reaction took place between the individual components.

### X-ray Diffraction Measurement

The phase identification of the composite gels was carried out by XRD analysis, and the XRD graphs of the HAp, CNC, and HAp/PVA/CNC composite gels were recorded to obtain a profile. As shown in Fig. 4(a), the main diffraction peaks in  $2\theta$  at 25.9, 31.8, 32.2, 34.1, and 40.0° were assigned to the (002), (211), (112), (202), and

(310) HAp indices according to the JCPDS file number 9-432 (Nassif *et al.* 2010), indicating that pure HAp particles were obtained by this chemical precipitation method. From Fig. 4(b), it was evident that two sharp peaks at the diffraction angle  $2\theta$  values of 16 and  $22.1^\circ$  could be attributed to the diffraction planes of (110) and (002), which is consistent with a typical cellulose I crystalline structure (Lu and Hsieh 2010). This result indicated that during the  $\text{NaClO}_2$  and sulfuric acid treatment, the amorphous and microcrystalline areas of the pulp fibers had been extensively destroyed, while the crystal structure of the CNC was not changed. The peaks at  $2\theta=19.4^\circ$  and  $2\theta=40.4^\circ$ , as can be seen in Fig. 4(c), were attributable to the characteristic crystalline peaks of PVA in the composite gels (Ricciardi *et al.* 2004). Furthermore, the peak at  $2\theta=19.4^\circ$  (101) was caused by the diffraction of the crystal plane of PVA, which was due to the intermolecular hydrogen bonding between PVA chains. However, these peaks were probably overlapped by the diffraction peaks of the HAp. Based on the above analysis, it was determined that the HAp/PVA/CNC composite gels were not formed by chemical reactions, but were probably formed due to physical hydrogen bonding. These results were well in agreement with the FT-IR analysis.

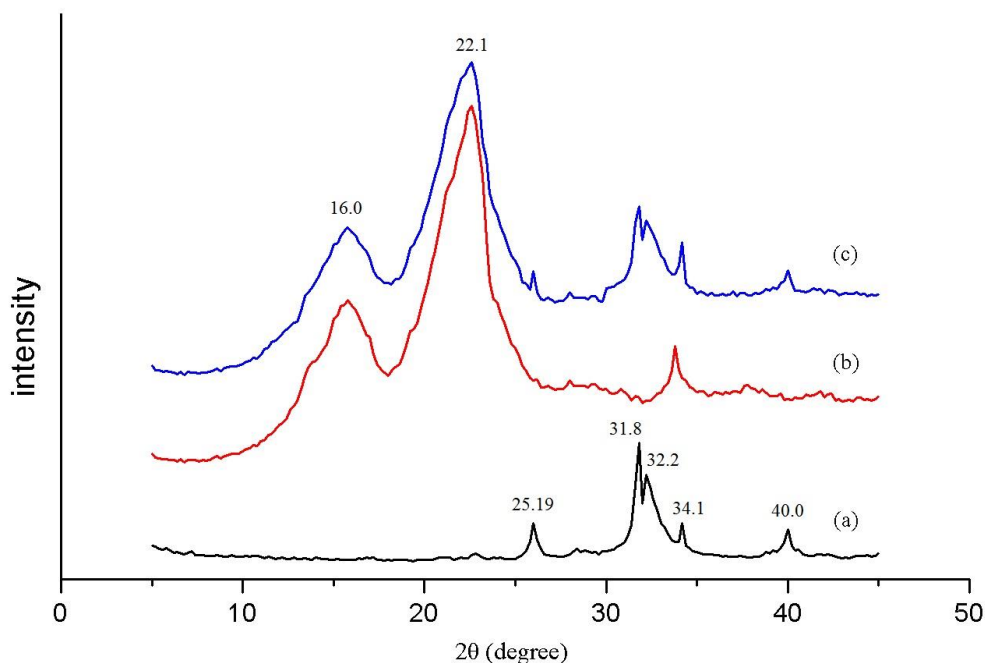
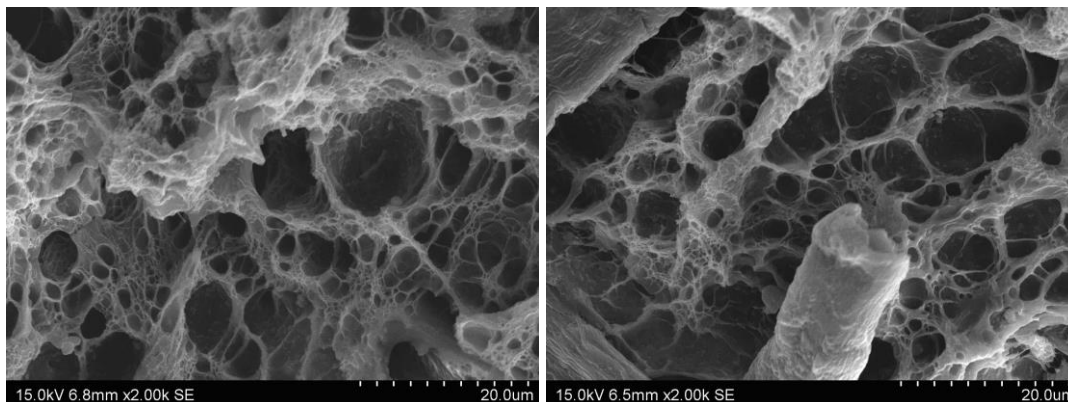


Fig. 4. XRD graphs of HAp (a), CNC (b), and HAp/PVA/CNC-3.75 composite gels (c)

### Morphology

To further understand the effect of the CNC on the morphology of the HAp/PVA composite gels, the morphological properties of the cross-sections of the samples were investigated via SEM, as shown in Fig. 4. The SEM images showed that the surfaces of the composites were highly porous in nature and indicated a resemblance to mesh. The size of the pores varied from 2 to 10  $\mu\text{m}$ , and all these pores formed a thoroughly interpenetrating network, which was beneficial for tissue growth and for the flow transport of nutrients and metabolic waste. As seen in Fig. 5(a), the inorganic HAp particles were uniformly distributed in the PVA matrix with no apparent signs of agglomeration, which is important for the final mechanical and biological performance of

this kind of particle-reinforced composite (Wang *et al.* 2001). Additionally, in contrast to the morphology of the HAp/PVA/CNC-0 composites, it was evident that the HAp/PVA/CNC-3.75 composites were surrounded or crossed by rod-shaped nanofibers, as illustrated in Fig. 5(b). The CNC were used as an enhancement phase in the interpenetrating polymer network, which could explain the fact that the mechanical properties of the HAp/PVA composites increased noticeably after the addition of CNC.



**Fig. 5.** SEM images of different composite gels as a function of CNC concentration. (a) represents the 0% CNC-HAp/PVA composite gels, and (b) represents the 3.75% CNC-HAp/PVA composite gels.

### Mechanical Properties

Adult cartilage is very high in tensile strength and modulus, offering integrity to the articular cartilage, and thus it is essential to study the tensile behavior of those composite gels used as articular cartilage replacement (Kempson 1979). The mechanical behavior of the composite gels depends significantly on the polymer structure and interstitial fluid, which is consistent with the behavior of articular cartilage (Kobayashi *et al.* 2005). Once a relatively small load is applied, the polymeric chains of the composite gels are reoriented, and their relative position is changed, leading to a significant deformation. If the application of the load continues, the reorientation of the chains tends to become uniform, which produces a hardening effect in the composite gels such that they require higher stress if they are to be deformed further (Ma *et al.* 2010; Maiolo *et al.* 2012). With this in mind, the HAp/PVA composite gels reinforced with different amounts of CNC were prepared so as to enhancing their mechanical properties.

The stress–strain characteristics of the prepared gels in the wet state are presented in Fig. 6, and the results for tensile strength, modulus and elongation at break are summarized in Table 1. It was clear that the stress–strain behaviors of all the composites gels exhibited an exponential pattern. Meanwhile, at the same strain level, the tensile stress of the composite gels increased with the increase in CNC. The tensile strength increased from 556.3 KPa for the 0% CNC-HAp/PVA composite gels to 2710.4 KPa for the 2.5% CNC-HAp/PVA composite gels, further to 3400.2 KPa for the 3.75% CNC-HAp/PVA composite gels, finally increased to 3756.9 KPa for the 6.25% CNC-HAp/PVA composite gels. Similarly, tensile modulus increased with increasing CNC content, and reached the highest value of 36.4 KPa at 6.25 wt% CNC. These results indicated that the CNC served as a reinforced phase and could significantly improve the mechanical properties of the HAp/PVA composite gels, probably due to the formation of

hydrogen bonding. Furthermore, the elongation at break of these composite gels could reach up to 150%, demonstrating that HAp/PVA/CNC composite gels had excellent ductility compared to normal elastic material. Finally, it should be noted that the stress-strain behavior of the HAp/PVA/CNC-0 appeared to have an almost linear pattern and had the lowest modulus and strain ratio, which was obviously different from those of composites reinforced with CNC. These results were in accordance with the conclusion concerning the tensile tests of swollen hydrogel addressed by Hassan and Peppas (2000).

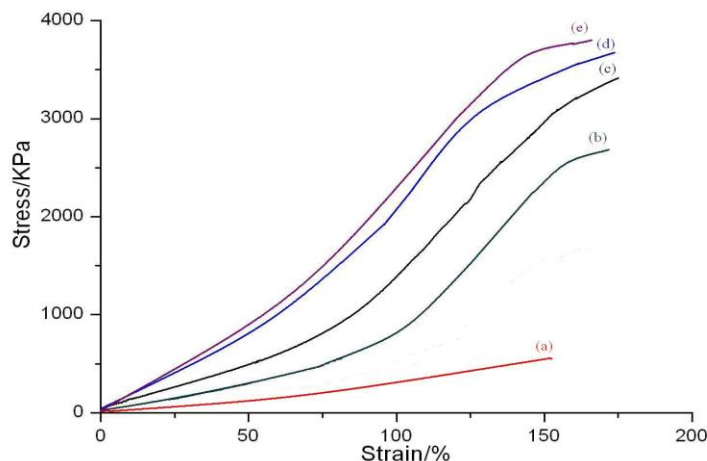


**Fig. 6.** Mechanical properties of different composite gels as a function of CNC concentration. (a) represents the 0% CNC-HAp/PVA composite gels; (b) represents the 2.5% CNC-HAp/PVA composite gels; (c) represents the 3.75% CNC-HAp/PVA composite gels; (d) represents the 5.0% CNC-HAp/PVA composite gels; and (e) represents the 6.25% CNC-HAp/PVA composite gels.

### Thermal Stability

To evaluate the thermal stability and understand the phase transformations of the prepared samples, thermogravimetric (TG) and derivative thermogravimetric (DTG) studies were performed in the range of 25 to 600 °C. The TG curves show weight loss in relation to the temperature of thermal degradation, while the DTG curves reveal the corresponding rate of weight loss. All the curves suggested that the addition of CNC had no significant effect on the thermal stability of the HAp/PVA composites.

As shown in Fig. 7(A), the samples had similar TG curves. It was clear that the sample weights started to decrease quickly when the decomposition temperature was around 300 °C. Moreover, the weight loss rate of the HAp/PVA composite was slightly greater than that of the HAp/PVA/CNC composite in the temperature range from 200 to 400 °C. However, after the decomposition temperature reached 400 °C, the weight loss rates showed the opposite trend. With regard to the whole decomposition process, the initial weight losses from 50 to 250 °C may have been due to the evaporation of surface adsorbed water molecules, while the quick weight loss from about 300 to 500 °C could be attributed to the endothermic dissociation of ions (Zheng *et al.* 1998). Furthermore, it should be pointed that the residue contents after decomposition were lower in sample (b) than in the sample (a), mainly due to the addition of the CNC. The DTG curves are shown in Fig. 7(B). As seen, the weight losses and maximum decomposition temperatures occurred mainly at two stages: one around 330 to 370 °C and the other around 440 °C. Sample (a) began to decompose at around 330 °C, whereas the

decomposition temperature for sample (b) was at 362 °C, probably due to the strong interaction between the CNC and HAp/PVA composites. In addition, the decomposition around 440 °C was attributed to the loss of  $\text{CO}_3^{2-}$  on the part of HAp (Jia *et al.* 2010).

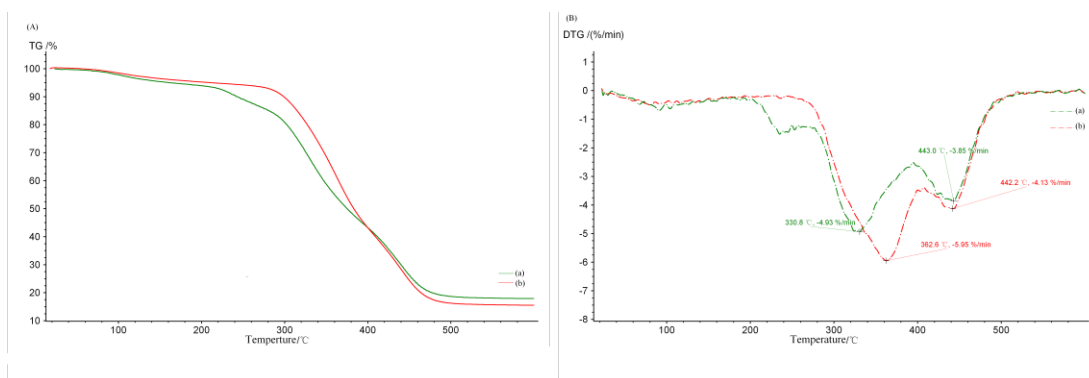


**Fig. 7.** Thermographical analysis of different composite gels as a function of CNC concentration. (a) represents the 0% CNC-HAp/PVA composite gels and (b) represents the 3.75% CNC-HAp/PVA composite gels.

**Table 1.** Mechanical Properties of Composite Gels with Different CNC Values

Samples <sup>a</sup>	Tensile strength [kPa]	Elongation [%]	Modulus [kPa]
(a)	556.3	158.5	3.2
(b)	2710.4	173.6	11.3
(c)	3400.2	177.9	27.5
(d)	3668.7	176.5	34.2
(e)	3756.9	169.5	36.4

<sup>a</sup>(a) represents the 0% CNC-HAp/PVA composite gels; (b) represents the 2.5% CNC-HAp/PVA composite gels; (c) represents the 3.75% CNC-HAp/PVA composite gels; (d) represents the 5.0% CNC-HAp/PVA composite gels; and (e) represents the 6.25% CNC-HAp/PVA composite gels.

## CONCLUSIONS

1. The HAp/PVA composite gels were prepared by adding HAp powder into a PVA solution and conducting freeze-thaw physical cross-linking.
2. Following CNC reinforcement, FT-IR and XRD profiles suggested that the new composite gels were formed only by physical hydrogen bonds, while the SEM images revealed that the CNC acted as an enhancement phase that interpenetrated into the network of the HAp/PVA composite gels. Furthermore, the mechanical properties were improved *via* the incorporation of these CNC into a polymer matrix, even at a low loading of 1.25%. In addition, the thermal stability of the HAp/PVA composites changed slightly after the addition of the CNC.
3. Consequently, in the future, strength-enhanced HAp/PVA/CNC composite gels may be good substitutes for the metal components of bone implants.

## ACKNOWLEDGMENTS

The authors are grateful for grants from the Beijing Municipal Natural Science Foundation (2122045), the Science & Technology Research Project of Guangxi University Education Department (2013YB321), the Wood Saving & Substitution Project (2013-3004), the Co-construction Project of Beijing Municipal Commission of Education of 2012, and the Beijing Municipal Co-construction Project of 2010.

## REFERENCES CITED

- Ahn, E. S., Gleason, N. J., Nakahira, A., and Ying, J. Y. (2001). "Nanostructure processing of hydroxyapatite-based bioceramics," *Nano. Lett.* 1(3), 149-153.
- Arvind, S., Gautam, D., and Binay, K. S. (2007). "Poly (vinyl alcohol) - hydroxyapatite biomimetic scaffold for tissue regeneration," *Mater. Sci. Eng. C.* 27(1), 70-74.
- Azizi Samir, M. A. S., Alloin, F., and Dufresne, A. (2005). "Review of recent research into cellulosic whiskers, their properties and their application in nanocomposite field," *Biomacromol.* 6(2), 612-626.
- Azizi Samir, M. A. S., Alloin, F., Sanchez, J. Y., Kissi, N. E., and Dufresne, A. (2004). "Preparation of cellulose whiskers reinforced nanocomposites from an organic medium suspension," *Macromol.* 37(4), 1386-1393.
- Balasundaram, G., and Webster, T. J. (2007). "An overview of nano-polymers for orthopedic applications," *Macromol. Biosci.* 7(5), 635-642.
- Bhattacharya, A., and Misra, B. N. (2004). "Grafting: A versatile means to modify polymers: Techniques, factors and applications," *Prog. Polym. Sci.* 29(8), 767-814.
- Candanedo, S. B., Roman, M., and Gray, D. G. (2005). "Effect of reaction conditions on the properties and behavior of wood cellulose nanocrystal suspensions," *Biomacromol.* 6(2), 1048-1054.
- Chiellini, E., Corti, A., D'Antone, S., and Solaro, R. (2003). "Biodegradation of poly (vinyl alcohol) based materials," *Prog. Polym. Sci.* 28(6), 963-1014.
- Du, C., Cui, F., Zhu, X., and Groot, K. (1999). "Three dimensional nano-HAp/collagen matrix loading with osteogenic cells in organ culture," *J. Biomed. Mater. Res.* 44(4), 407-415.
- Eichhorn, S. J. (2011). "Cellulose nanowhiskers: Promising materials for advanced applications," *Soft Matter* 7(2), 303-315.
- Gonzalez, J. S., and Alvarez V. A. (2014). "Mechanical properties of polyvinyl alcohol/hydroxyapatite cryogel as potential artificial cartilage," *J. Mech. Behav. Biomed. Mater.* 34, 47-56.
- Habibi, Y., Lucia, L. A., and Rojas, O. J. (2010). "Cellulose nanocrystals: Chemistry, self-assembly, and applications," *Chem. Rev.* 110(6), 3479-3500.
- Hassan, C. M., and Peppas, N. A. (2000). "Structure and morphology of freeze/thawed PVA hydrogels," *Macromol.* 33(7), 2472-2479.
- He, M., Chang, C. Y., Peng, N., and Zhang, L. N. (2012). "Structure and properties of hydroxyapatite/cellulose nanocomposite films," *Carbohydr. Polym.* 87(4), 2512-2518.
- Huang, H. Y., Liu, Z. H., and Tao, F. (1997). "In vivo evaluation of porous hydroxyapatite ceramic as cervical vertebra substitute," *Clin. Neurol. Neurosurg.* 99(S1), 20-21.

- Hyon, S. H., Cha, W. I., and Ikada, Y. (1989). "Preparation of transparent poly (vinyl alcohol) hydrogel," *Polym. Bull.* 22(2), 119-122.
- Jia, N., Li, S. M., Ma, M. G., Sun, R. C., and Zhu, J. F. (2010). "Hydrothermal synthesis and characterization of cellulose-carbonated hydroxyapatite nanocomposites in NaOH-urea aqueous solution," *Sci. Adv. Mater.* 2(2), 210-214.
- Kempson, G. E. (1979). "Mechanical properties of articular cartilage," in: *Adult Articular Cartilage*, M. A. R. Freeman (ed.), Pitman Medical, London, pp. 333-414.
- Kobayashi, M., Chang, Y. S., and Oka, M. (2005). "A two year *in vivo* study of polyvinyl alcohol-hydrogel (PVA-H) artificial meniscus," *Biomaterials* 26(16), 3243-3248.
- Lu, P., and Hsieh, Y. L. (2010). "Preparation and properties of cellulose nanocrystals: Rods, spheres, and network," *Carbohydr. Polym.* 82(2), 329-336.
- Ma, R., Xiong, D., Miao, F., Zhang, J., and Peng, Y. (2010). "Novel PVP/PVA hydrogels for articular cartilage replacement," *Mater. Sci. Eng. C.* 29(6), 1979-1983.
- Maiolo, A. S., Amado, M. N., Gonzalez, J. S., and Alvarez, V. A. (2012). "Development and characterization of Poly (vinyl alcohol) based hydrogels for potential use as an articular cartilage replacement," *Mater. Sci. Eng. C.* 32(6), 1490-1495.
- Nassif, N., Martineau, F., Syzgantseva, O., Gobeaux, F., Willinger, M., and Coradin, T. (2010). "*In vivo* inspired conditions to synthesize biomimetic hydroxyapatite," *Chem. Mater.* 22(12), 3653-3663.
- Pan, Y., Xiong, D., and Chen, X. (2007). "Friction characteristics of poly (vinyl alcohol) hydrogel as an articular cartilage biomaterial," *Key Eng. Mater.* 330-332, 1297-1300.
- Pan, Y., and Xiong, D. (2010). "Preparation and characterization of nano-hydroxyapatite/polyvinyl alcohol gel composites," *J. Wuhan Univ. Technol. - Mater. Sci. Ed.* 25(3), 474-478.
- Pushpakanth, S., Srinivasan, B., Sreedhar, B., and Sastry, T. P. (2008). "An *in situ* approach to prepare nanorods of titania-hydroxyapatite (TiO<sub>2</sub>-HAp) nanocomposite by microwave hydrothermal technique," *Mater. Chem. Phys.* 107(2-3), 492-498.
- Ricciardi, R., Auriemma, F., de Rosa, C., and Laupretre, F. (2004). "X-ray diffraction analysis of poly(vinyl alcohol) hydrogels, obtained by freezing and thawing techniques," *Macromol.* 37(5), 1921-1927.
- Siqueira, G., Bras, J., and Dufresne, A. (2009). "Cellulose whiskers versus microfibrils: Influence of the nature of the nanoparticle and its surface functionalization on the thermal and mechanical properties of nanocomposites," *Biomacromol.* 10(2), 425-432.
- Stammen, J. A., Williams, S., Ku, D. N., and Guldberg, R. E. (2001). "Mechanical properties of a novel PVA hydrogel in shear and unconfined compression," *Biomaterials* 22(8), 799-806.
- Sun, X. X., and Uyama, H. (2014). "In situ mineralization of hydroxyapatite on poly(vinyl alcohol) monolithic scaffolds for tissue engineering," *Colloid Polym. Sci.* 292, 1073-1078.
- Swetha, M., Sahithi, K., Moorthi, A., Srinivasan, N., Ramasamy, K., and Selvamurugan, N. (2010). "Biocomposites containing natural polymers and hydroxyapatite for bone tissue engineering," *Int. J. Biol. Macromol.* 47(1), 1-4.
- Wang, M., Chen, L. J., Ni, J., Weng, J., and Yue, C. Y. (2001). "Manufacture and evaluation of bioactive and biodegradable materials and scaffolds for tissue engineering," *J. Mater. Sci. Mater. Med.* 12(10-12), 855-860.

- Wu, G., Su, B., Zhang, W. G., and Wang, C. T. (2008). “*In vitro* behaviors of hydroxyapatite reinforced polyvinyl alcohol hydrogel composite,” *Mater. Chem. Phys.* 107(2-3), 364-369.
- Zhang, D., Duan, J., Wang, D., and Ge, S. (2010). “Effect of preparation methods on mechanical properties of PVA/HA composite hydrogel,” *J. Bionic Eng.* 7(3), 235-243.
- Zheng, G., Jiu, X., and Xiang, Z. (1998). “The development of artificial articular cartilage-PVA-hydrogel,” *Biomed. Mater. Eng.* 8(2), 75-81.

Article submitted: November 12, 2013; Peer review completed: April 13, 2014; Revised version received and accepted: August 15, 2014; Published: August 20, 2014.